1018 *Organometallics* **2003,** *22,* 1018−1028

(Ethene)bis(acetylacetonato) Complexes of Divalent and Trivalent Ruthenium

Martin A. Bennett,* Matthew J. Byrnes, and Anthony C. Willis

Research School of Chemistry, Australian National University, Canberra, ACT 0200, Australia

Received September 30, 2002

Downloaded by CARLI CONSORTIUM on June 29, 2009
Published on January 30, 2003 on http://pubs.acs.org | doi: 10.1021/om020815b

Zinc dust reduction of tris(acetylacetonato)ruthenium(III), [Ru(acac)$_3$], in hot aqueous THF in the presence of ethene gives *cis*-[Ru(acac)$_2$(η^2-C_2H_4)$_2$] (**5**), isolated as an orange solid in ca. 60% yield. A single-crystal X-ray crystallographic study shows the metal atom to be coordinated octahedrally by a pair of bidentate O-bonded acac groups and two mutually *cis* orthogonal ethene ligands. In the NMR spectra of **5**, the ethene carbon atoms remain equivalent, while the protons are inequivalent in pairs, down to −95 °C; intermolecular exchange with ethene is slow on the NMR time scale at room temperature but becomes fast above ca. 80 °C. One of the ethene molecules of **5** is replaced by ligands at room temperature to give [Ru(acac)$_2$(η^2-C_2H_4)(L)] [L = $SbPh_3$ (**6**), MeCN (**7**), NH_3 (**8**), and C_5H_5N (**9**)]. Complexes **6** and **7** are isolated as *cis*-isomers, **9** as a *cis*−*trans* mixture, and **8** in the form of the *trans*-isomer which transforms into the *cis*-isomer when heated or chromatographed on alumina. The structures of *cis*-**8** and *trans*-**9** have been confirmed by X-ray crystallography. The results indicate that ligand substitutions on **5** may occur via a square pyramidal intermediate [Ru(acac)$_2$(η^2-C_2H_4)] in which ethene occupies the apical site. All the complexes display either a quasi-reversible or a fully reversible one-electron oxidation by cyclic voltammetry at −50 °C, with $E_{1/2}$ values in the range +0.37−0.59 V for **6**−**9** and +0.95 V for **5** (in 0.5 M [Bu_4N]PF_6/CH_2Cl_2 vs Ag/AgCl/MeCN). The blue oxidized species **5**$^+$, **6**$^+$, and **8**$^+$ can be generated by bulk electrolysis and are stable for hours at −50 °C. Their UV−vis spectra and the ESR spectra of **6**$^+$ and **8**$^+$ indicate that the oxidized species are ruthenium(III)-ethene cations. Oxidation of the known cyclooctene complex *cis*-[Ru(acac)$_2$(η^2-C_8H_{14})($SbPh_3$)] (**2**) with $AgPF_6$ at −50 °C gives an isolable, deep blue ruthenium(III) salt [**2**]$^+$[PF_6]$^-$, which is stable at room temperature.

Introduction

Among mononuclear dipositive d-block metal ions, ruthenium(II) is notable for the ability of its classical coordination complexes containing typical hard ligands such as H_2O and NH_3 to bind soft, π-acceptor ligands.[1,2] This property is manifest, for example, in the existence of stable, cationic alkene complexes such as [Ru(NH_3)$_5$(η^2-C_2H_4)]$^{2+}$,[3] [Ru(NH_3)$_4$(*s-trans*-η^4-C_4H_6)]$^{2+}$,[4] [Ru(H_2O)$_5$(η^2-C_2H_4)]$^{2+}$,[5] and [Ru(H_2O)$_4$(η^2-C_2H_4)$_2$]$^{2+}$.[5] The presence of π-acceptor ligands in the coordination sphere tends to stabilize the occupied metal π-orbitals (HOMO) and reduce the interelectronic repulsion in the metal ion, thus stabilizing Ru(II) $\{t_{2g}^6\}$ relative to $Ru^{III}\{t_{2g}^5\}$. Thus, the reduction potentials $E_{1/2}$ of the $Ru^{3+/2+}$ couple for [Ru(NH_3)$_5$(η^2-alkene)]$^{2+}$ complexes range from +0.83 V (alkene = propene)[6] to 0.98 V (alkene = styrene)[7] vs NHE in aqueous solution, corresponding to a stabilization at the Ru(II) level of ca. 0.75 V compared to [Ru(NH_3)$_6$]$^{2+}$ ($E_{1/2}$ = +0.05 V vs NHE).[8] A similar trend is evident in the $E_{1/2}$ values for the aqua-ions [Ru(H_2O)$_6$]$^{2+}$ (+0.19 V vs NHE)[9] and [Ru(H_2O)$_5$(η^2-C_2H_4)]$^{2+}$ (+0.84 V vs NHE).[10] The electrogenerated one-electron oxidation products [Ru(NH_3)$_5$(η^2-alkene)]$^{3+}$ cannot be isolated or detected because the coordinated alkene is rapidly replaced by the solvent (water) in which the cyclic voltammetry is carried out.[6,7,11] In the closely related osmium series, however, the alkyne-osmium(III) species [Os(NH_3)$_5$(η^2-PhC≡CPh)](PF_6)$_3$ has been isolated by oxidation of [Os(NH_3)$_5$(η^2-PhC≡CPh)](OTf)$_2$ with [$FeCp_2$]PF_6.[12]

We have been investigating the binding of π-acceptor ligands to the bis(acetylacetonato)ruthenium(II) fragment [acetylacetonato (acac) = 2,4-pentanedionato, $C_5H_7O_2$] in the expectation that the presence of this anionic O-donor in the coordination sphere would help to stabilize the trivalent relative to the divalent state and allow ruthenium(III)-alkene complexes to be iso-

---

(1) Taube, H. *Comments Inorg. Chem.* **1981**, *1*, 17.

(2) Grundler, P. V.; Laurenczy, G.; Merbach, E. *Helv. Chim. Acta* **2001**, *84*, 2854.

(3) Lehman, H.; Schenk, K. J.; Chapuis, G.; Ludi, A. *J. Am. Chem. Soc.* **1979**, *101*, 6197.

(4) Sugaya, T.; Tomita, A.; Sago, H.; Sano, M. *Inorg. Chem.* **1996**, *35*, 2692.

(5) Laurenczy, G.; Merbach, A. E. *J. Chem. Soc., Chem. Commun.* **1993**, 187.

(6) Elliott, M. G.; Shepherd, R. E. *Inorg. Chem.* **1988**, *27*, 3332.

(7) Elliott, M. G.; Zhang, S.; Shepherd, R. E. *Inorg. Chem.* **1989**, *28*, 3036.

(8) Lim, H. S.; Barclay, D. J.; Anson, F. C. *Inorg. Chem.* **1972**, *11*, 1460.

(9) McGrath, D. V.; Grubbs, R. H.; Ziller, J. W. *J. Am. Chem. Soc.* **1991**, *113*, 3611.

(10) Aebischer, N.; Sidorenkova, E.; Ravera, M.; Laurenczy, G.; Osella, D.; Weber, J.; Merbach, A. E. *Inorg. Chem.* **1997**, *36*, 6009.

(11) Zhang, S.; Shepherd, R. E. *Inorg. Chim. Acta* **1989**, *163*, 237.

(12) Harman, W. D.; Wishart, J. F.; Taube, H. *Inorg. Chem.* **1989**, *28*, 2411.

10.1021/om020815b CCC: $25.00 © 2003 American Chemical Society
Publication on Web 01/30/2003

Downloaded by CARLI CONSORTIUM on June 29, 2009
Published on January 30, 2003 on http://pubs.acs.org | doi: 10.1021/om020815b

Scheme 1

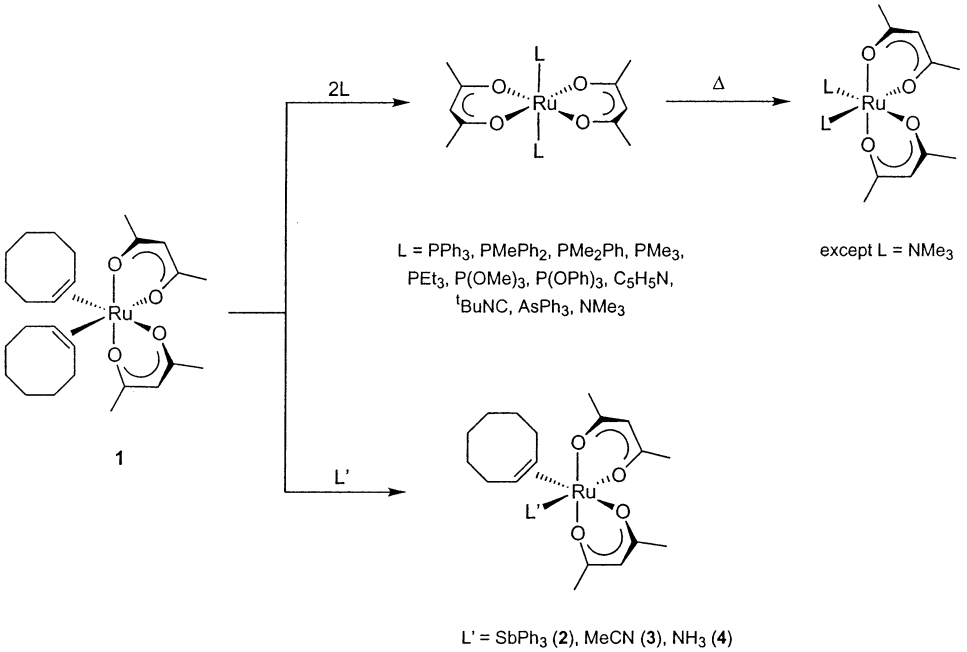

Scheme 2

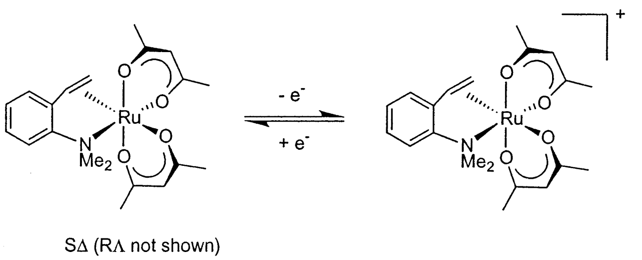

Scheme 3

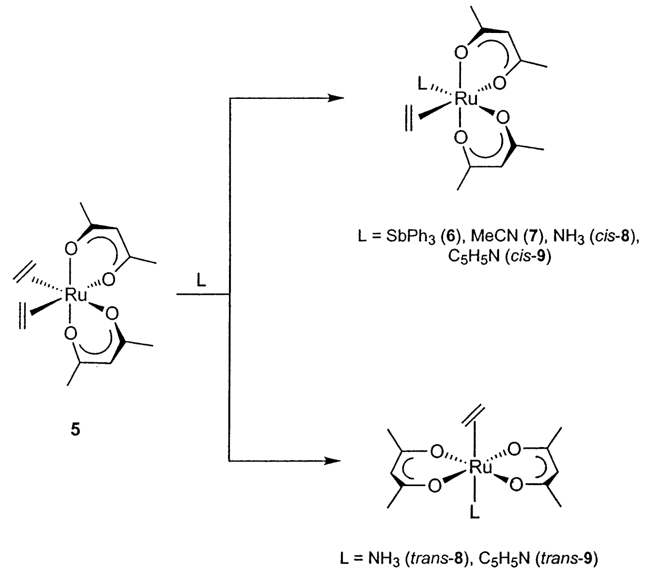

lated or at least detected. We found that reduction of [Ru(acac)$_3$] with zinc in aqueous THF containing cyclooctene (C_8H_{14}) gives a solution containing *cis*-[Ru(acac)$_2$(η^2-C_8H_{14})$_2$] (**1**), which cannot be isolated and is stable only in the presence of an excess of cyclooctene.[13] The alkene ligands are displaced by many ligands (L) (e.g., tertiary phosphines, phosphites, triphenylarsine, pyridine, and *tert*-butyl isocyanide) to give *trans*-[Ru(acac)$_2$L$_2$] as kinetic products, which then usually isomerize to the more stable *cis*-isomers on heating (Scheme 1). Only in the cases of triphenylstibine, acetonitrile, and ammonia (L′) could monosubstitution products, *cis*-[Ru(acac)$_2$(η^2-C_8H_{14})(L′)] (**2**−**4**), be obtained. Ruthenium(II) complexes of chelating unsaturated tertiary amines, such as [Ru(acac)$_2$(*o*-CH$_2$=CHC$_6$H$_4$-NMe$_2$)] (Scheme 2), have been obtained similarly from [Ru(acac)$_3$] and shown to undergo one-electron oxidation to the corresponding structurally authenticated complexes of ruthenium(III).[14,15] The latter provide unusual examples of alkene coordination to a paramagnetic metal center in a fairly high oxidation state.

In extending this work, we wished, if possible, to isolate and structurally characterize the ethene analogue of **1**, *cis*-[Ru(acac)$_2$(η^2-C_2H_4)$_2$] (**5**), and to study its reactions with ligands in order to establish the stereochemical course of the first step in the substitution of the coordinated alkene. It was also hoped that one-electron oxidation of some of the monosubstitution products [Ru(acac)$_2$(η^2-alkene)(L)] might give isolable or detectable ruthenium(III)-alkene complexes that were not stabilized by the chelate effect.

Results

The preparation and reactions of *cis*-[Ru(acac)$_2$(η^2-C_2H_4)$_2$] (**5**) are summarized in Scheme 3. Selected infrared bands, mass spectrometric data, and elemental analyses for the new complexes are given in Table 1; ^{1}H and ^{13}C{^{1}H} NMR data are listed in Table 2.

Ruthenium(II) Complexes. Reduction of [Ru(acac)$_3$] in hot, aqueous THF with freshly activated zinc dust under ethene (3 bar) gave an orange solution from which complex **5** was isolated as a moderately air-stable

---

[13] Bennett, M. A.; Chung, G.; Hockless, D. C. R.; Neumann, H.; Willis, A. C. *J. Chem. Soc., Dalton Trans.* **1999**, 3451.

[14] Bennett, M. A.; Heath, G. A.; Hockless, D. C. R.; Kovacik, I.; Willis, A. C. *J. Am. Chem. Soc.* **1998**, *120*, 932.

[15] Bennett, M. A.; Heath, G. A.; Hockless, D. C. R.; Kovacik, I.; Willis, A. C. *Organometallics* **1998**, *17*, 5867.

Downloaded by CARLI CONSORTIUM on June 29, 2009
Published on January 30, 2003 on http://pubs.acs.org | doi: 10.1021/om020815b

Table 1. Elemental Analyses, Selected Infrared Bands, and Mass Spectra of Ruthenium-Alkene Complexes

	analysis [calcd (found)]			IR (cm^{-1}, KBr)		
	%C	%H	%other	ν(acac)	other	*m*/*z* (intensity %, assignment)
5[a]	47.3 (47.1)	6.2 (5.9)		1576, 1515		356.0 (10, M), 328.0 (23, $M-C_2H_4$), 299.9 (100, $M-2C_2H_4$)
6[b]	53.0 (53.4)	4.9 (4.8)		1568, 1514		679.9 (19, M), 653.9 (100, $M-C_2H_4$), 552.9 (25, $M-C_2H_4-$acac), 299.9 (97, Ru(acac)$_2$)
7	45.65 (45.4)	5.75 (6.0)	3.8 (3.4) (N)	1571, 1518	2262 [ν(CN)]	369.0 (23, M), 349.0 (54, $M-C_2H_4$), 299.9 (100, Ru(acac)$_2$)
trans-**8**	41.85 (41.7)	6.15 (6.1)	4.1 (4.1) (N)	1567, 1510	3335 [$\nu(NH_3)$]	345.0 (45, M), 317.0 (77, $M-C_2H_4$), 299.9 (100, Ru(acac)$_2$)
cis-**8**	41.85 (41.8)	6.15 (5.9)	4.1 (4.1) (N)	1566, 1510	3334 [$\nu(NH_3)$]	345.0 (92, M), 317.0 (100, $M-C_2H_4$), 300.0 (87, Ru(acac)$_2$)
9[c]	50.2 (52.8)	5.7 (5.9)	3.45 (2.9) (N)	1565, 1515		407.1 (9, M), 379.1 (100, $M-C_2H_4$), 300.1 (85, Ru(acac)$_2$)
[**2**]PF_6[d−f]	46.35 (46.3)	4.65 (4.8)	3.65 (3.3) (P)	1552, 1518	840, 557 [$\nu(PF_6)$]	762.2 (80, M), 652.1 (100, $M-C_8H_{14}$), 300.0 (100, Ru(acac)$_2$)

[a] FAB-MS also shows peaks at *m*/*z* 579.1 (2) and 551.1 (20) arising from reaction with the matrix. [b] FAB-MS also shows a peak at *m*/*z* 1005.9 (8) due to $[Ru(acac)_2(SbPh_3)_2]$. [c] Compound appears to be pure according to NMR (^1H, ^{13}C) spectra; the reason for the poor C and N analyses is unknown. [d] Calcd values refer to [**2**]PF_6 containing 10% $AgPF_6$. [e] %Ag: calcd 1.60, found 1.16. [f] FAB-MS also shows a peak at *m*/*z* 1006.2 (15) due to $[Ru(acac)_2(SbPh_3)_2]$.

Table 2. ^1H and $^{13}C\{^1H\}$ NMR Data for Complexes 5−9[a]

	^1H			^{13}C			
		acac			acac		
	C_2H_4	γ-CH	CH_3	C_2H_4	C=O	γ-C	CH_3
5	3.85−3.70 (m, 8H)	5.24 (s, 2H)	1.86, 1.82 (each s, 6H)	78.2	186.6, 185.1	98.0	27.5, 26.9
6[b]	4.26−3.99 (m, 4H)	5.30, 5.15 (each s, 1H)	2.02, 1.74, 1.69, 1.62 (each s, 3H)	57.9	188.7, 186.8, 185.8, 185.3	100.2, 98.6	28.0, 27.9, 27.7, 27.4
7[c]	4.44−4.37 (m, 4H)	5.50, 5.29 (each s, 1H)	2.17, 2.01, 2.00, 1.81 (each s, 3H)	72.5	187.8, 186.8, 185.8, 185.3	99.1, 99.0	28.2, 27.9, 27.7, 27.3
trans-**8**[d,e]	3.70 (s, 4H)	5.38 (s, 2H)	1.91 (s, 12H)	72.2	186.9	99.6	27.8
cis-**8**[f]	4.30−4.10 (m, 4H)	5.28, 5.14 (each s, 1H)	2.35, 2.18, 2.02, 1.97 (each s, 3H)	65.9	189.1, 185.6, 185.5, 184.0	99.1, 98.9	28.1, 28.0, 27.7, 27.4
trans-**9**[g]	4.29 (s, 4H)	5.05 (s, 2H)	1.80 (s, 12H)	75.4	186.0	99.5	27.7
cis-**9**[h]	4.29 (s, 4H)	5.33, 5.32 (each s, 1H)	1.96, 1.94, 1.90, 1.88 (each s, 3H)	73.1	187.6, 186.4, 185.8, 185.0	99.3, 99.2	28.4, 28.1, 27.9, 27.6

[a] In C_6D_6 at 300 MHz (^1H), 75.4 MHz (^{13}C), except where stated. [b] ^1H: δ 7.70−7.67 (m, 6H), 7.13−7.00 (m, 9H); ^{13}C: δ 136.6, 132.0, 129.6, 128.9 (Ph_3Sb). [c] ^1H: δ 0.59 (s, 3H, MeCN); ^{13}C: δ 2.1 (*Me*CN); Me*C*N was not located. [d] Measured in CD_2Cl_2. [e] ^1H: δ 3.05 (br s, 3H, NH_3). [f] ^1H: δ 1.52 (br s, 3H, NH_3). [g] ^1H: δ 8.85 (d, 1H, $J = 5$ Hz), 6.82 (d, 2H, $J = 7$ Hz), 6.66 (d, 2H, $J = 7$ Hz); ^{13}C: δ 151.9, 136.7, 123.6 (C_5H_5N). [h] ^1H: δ 8.53 (d, 1H, $J = 5$ Hz), 6.64 (d, 2H, $J = 7$ Hz), 6.38 (d, 2H, $J = 7$ Hz); ^{13}C: δ 153.6, 134.3, 123.3 (C_5H_5N).

orange solid in ca. 60% yield. Solutions in benzene, toluene, and THF are stable in the absence of air, whereas dichloromethane solutions decompose slowly at ca. 20 °C. The solid turns violet after several weeks' exposure to air. The strongest peak in the isotopic pattern in the positive FAB-mass spectrum of **5** is due to the parent ion; there are also peaks arising from the successive loss of two ethene molecules. The IR spectrum of **5** shows two strong bands, characteristic of bidentate, O-bonded acac,[16] at 1576 and 1515 cm^{-1}, beneath which the ν(C=C) band of coordinated C_2H_4 is probably concealed; by analogy with spectra reported for the $[Ru(NH_3)_5(\eta^2\text{-alkene})]^{2+}$ complexes, it would be expected to appear in the range 1550−1490 cm^{-1}.[3]

In the ^1H and $^{13}C\{^1H\}$ NMR spectra of **5**, the acac groups give rise to two methyl singlets, one methine singlet, and two carbonyl resonances, consistent with the presence of a *cis*-$[Ru(acac)_2]$ moiety attached to two identical ligands. The ethene protons appear as an 8H-AA′BB′ multiplet at δ 3.70−3.85, the nonequivalence presumably arising because the *cis*-$[Ru(acac)_2]$ fragment is prochiral. The ca. 2 ppm shift to low frequency compared with the value for free ethene (δ 5.24) is similar to that found in $[Ru(NH_3)_5(\eta^2\text{-}C_2H_4)]^{2+}$ (δ 3.57)[3] and *cis*-$[Ru(H_2O)_4(\eta^2\text{-}C_2H_4)_2]^{2+}$ (δ 3.81).[5] A similar shift has also been noted for the olefinic hydrogen atoms in *cis*-$[Ru(acac)_2(\eta^2\text{-}C_8H_{14})_2]$ (**1**).[13] A signal at δ 78.2 (J_{CH} = 160 Hz) is assigned to the ethene carbon atoms of **5**.

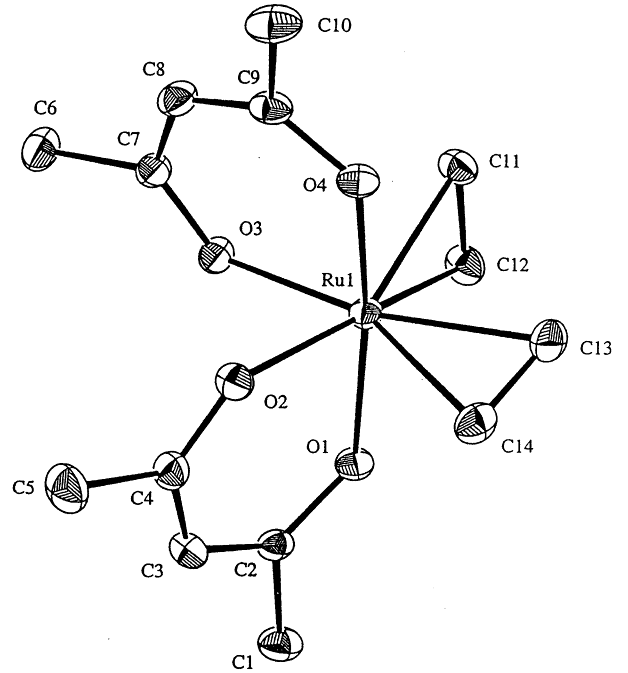

Figure 1. Molecular structure of *cis*-$[Ru(acac)_2(\eta^2\text{-}C_2H_4)_2]$ (**5**) with selected atom labeling. Thermal ellipsoids show 30% probability levels; hydrogen atoms have been omitted for clarity.

The single-crystal X-ray structure of **5**, which is shown in Figure 1 and discussed in detail below, shows that the metal atom lies at the center of a distorted

---

(16) Nakamoto, K. *Infrared and Raman Spectra of Inorganic and Coordination Compounds*, 5th ed.; Wiley: New York, 1997; Part B, p 91.

Downloaded by CARLI CONSORTIUM on June 29, 2009
Published on January 30, 2003 on http://pubs.acs.org | doi: 10.1021/om020815b

octahedron formed by two *cis*-acac groups and two *cis*-ethene molecules. The latter are mutually orthogonal, and if this static structure were preserved in solution, one would have expected inequivalence of all the ethene carbon atoms and a more complex pattern for the ethene proton signals. The simpler pattern observed suggests that the ethene ligands are rotating rapidly about the Ru−C_2H_4 bonds at room temperature, thus equilibrating mutually *trans*-positions in the ethene ligands. A similar situation has been reported recently for the chiral complex $[Pt(\eta^2\text{-}C_2H_4)\{cis\text{-}1\text{-}(N{=}CHC_6H_4)\text{-}2\text{-}(N{=}CHPh)C_6H_{10}\}]^+$.[17] When a solution of **5** was cooled to −95 °C, the $^{13}C\{^1H\}$ resonance of coordinated ethene remained sharp while the two halves of the symmetrical proton multiplet moved apart[18] and broadened slightly. At room temperature the ethene proton multiplet did not broaden in the presence of free ethene; hence, in contrast to the behavior of the rhodium(I) complex $[Rh(acac)(\eta^2\text{-}C_2H_4)_2]$,[19] intermolecular exchange is slow on the NMR time scale.

When a solution of **5** was heated in toluene-d_8 to ca. 95 °C, the ethene proton multiplets converged to a broad singlet at δ 3.64. Above ca. 60 °C a number of low-intensity peaks also appeared, arising from irreversible decomposition. In the presence of free ethene, there was no observable decomposition, but the behavior of the ethene proton multiplet was identical, the estimated coalescence temperature being ca. 80 ± 5 °C. Broadening of the acac methyl and free ethene singlets became evident above ca. 90 °C, and the latter also shifted to higher frequency, suggestive of rapid intermolecular exchange of free and coordinated ethene under these conditions. In view of the complexity of the ethene proton spin system and the small chemical shift difference, we have not attempted a quantitative treatment of the data based on line-shape analysis.

One of the coordinated ethene molecules of **5** was readily replaced by certain ligands at room temperature to give the complexes $[Ru(acac)_2(\eta^2\text{-}C_2H_4)(L)]$ [L = $SbPh_3$ (**6**), MeCN (**7**), NH_3 (**8**), or py (**9**)], which were isolated as yellow or brown air-stable solids in yields of 60−80%. They display parent ion peaks in their FAB-mass spectra and the usual strong IR bands due to bidentate O-bonded acac. In their ^1H and $^{13}C\{^1H\}$ NMR spectra, complexes **6** and **7** show four acac methyl and two acac γ-CH resonances, and there are four acac C=O resonances in the region δ 180−190; hence, these compounds are *cis*-isomers. Similar data have been reported for the cyclooctene-triphenylstibine and -acetonitrile complexes, **2** and **3**, respectively,[13] and for *cis*-$[Ru(acac)_2(\eta^2\text{-}C_2H_4)(SbPr^i_3)]$.[20] The presence of coordinated acetonitrile in **7** is evident from the IR and NMR spectra.

The reaction of **5** with an excess of dry ammonia gas in THF gave *trans*-$[Ru(acac)_2(\eta^2\text{-}C_2H_4)(NH_3)]$ (*trans*-**8**), which is almost insoluble in benzene, toluene, ether, and acetone, and shows equivalent acac CH_3, CH, and C=O groups in its ^1H and $^{13}C\{^1H\}$ NMR spectra in CD_2Cl_2. It isomerized to the more soluble *cis*-compound when its solution in CH_2Cl_2 was passed through a column of neutral alumina (Activity III) or, more slowly, when a solution in CD_2Cl_2 was kept at room temperature. The structure of *cis*-**8** follows from the NMR spectroscopic data and has been confirmed by X-ray crystallography (see below). The proton chemical shifts of coordinated ammonia differ considerably for the two isomers (δ 3.05 and 1.52 for *trans*-**8** and *cis*-**8**). Both isomers show a band of medium intensity at ca. 3335 cm^{-1} due to the antisymmetric NH_3 stretching mode, and for the *cis*-isomer, a band at 1626 cm^{-1} assignable to an NH_3 deformation mode could also be located.[21]

Reaction of **5** with an equimolar amount of pyridine in benzene at room temperature gave a 3:2 ratio of *cis*- and *trans*-**9**, as estimated from the ^1H and $^{13}C\{^1H\}$ NMR spectra. An X-ray quality crystal of *trans*-**9** was obtained from an attempted fractional crystallization; the structure is discussed below. Complete conversion into *cis*-**9** occurred on heating the mixture overnight in benzene-d_6, but in refluxing toluene partial decomposition occurred, giving *cis*-$[Ru(acac)_2py_2]$.[13]

As expected, the ethene protons of *trans*-**8** and *trans*-**9** appear as sharp 4H singlets, whereas those of **6**, **7**, and *cis*-**8** at room temperature give rise to symmetrical 4H multiplets in the region δ 4.5−4.0 whose patterns resemble that of the corresponding protons in **5** and those found at low temperature for $[Rh(acac)(\eta^2\text{-}C_2H_4)_2]$[22] and $[Rh(\eta^5\text{-}C_5H_5)(\eta^2\text{-}C_2H_4)(L)]$ {L = C_2H_4,[19,22] C_2F_4,[22] or SO_2[22]}. Surprisingly, the ethene proton resonance of *cis*-**9** is a singlet. The ethene carbon atoms occur as singlets in the region of δ 70 for all the complexes. Presumably ethene rotation is fast in all cases, and although the ^1H multiplet for **6** broadens at ca. −90 °C into two featureless peaks, it is not clear whether this is due to slowed ethene rotation.

X-ray Structures of *cis*-[Ru(acac)$_2$(η^2-C$_2$H$_4$)(L)] [L = C$_2$H$_4$ (5), NH$_3$ (8)] and *trans*-[Ru(acac)$_2$(η^2-C$_2$H$_4$)(py)] (*trans*-9). The molecular geometries are shown in Figures 1−3, and selected metrical parameters are listed in Tables 3−5, respectively. In all three compounds the ruthenium atom is essentially octahedrally coordinated if the midpoint of the C=C bond is taken as the donor center. In **5** the dihedral angle between the planes defined by the metal atom and the carbon atoms of each ethene ligand, Ru(1)−C(11)−C(12) and Ru(1)−C(13)−C(14), is 90°. The plane defined by the atoms Ru(1)−C(11)−C(12) also eclipses that defined by the atoms Ru(1)−O(1)−O(4). The ethene hydrogen atoms are bent away from the metal center forming an angle α of 26−36°, α being defined as the angle between the normals to the H−C−H planes.[23] In *cis*-**8** the C=C vector of the ethene eclipses the Ru(1)−O(2)−N(1) plane, whereas *trans*-**9** is disordered such that the ethene ligand occupies two, mutually orthogonal orientations that eclipse the Ru−O bonds. The ethene C=C distances in all three compounds are ca. 1.35−1.37 Å, i.e., slightly greater than that in free ethene [1.337(2) Å]. The Ru−C distances in **5** [2.183(2)−2.212(2) Å] appear to be significantly greater than those in *cis*-**8** [2.147(3), 2.151(3) Å] and in the diastereomeric chelate complexes [Ru-

---

[17] Baar, C. R.; Jenkins, H. A.; Jennings, M. C.; Yap, G. P. A.; Puddephatt, R. J. *Organometallics* **2000**, *19*, 4870.

[18] The separation between the more intense inner lines of the multiplet increases from 7.8 Hz at 268 K to 26.4 Hz at 183 K.

[19] Cramer, R. *J. Am. Chem. Soc.* **1964**, *86*, 217.

[20] Grünwald, G.; Laubender, M.; Wolf, J.; Werner, H. *J. Chem. Soc., Dalton Trans.* **1998**, 833.

[21] Reference 16, p 6.

[22] Cramer, R.; Kline, J. B.; Roberts, J. D. *J. Am. Chem. Soc.* **1969**, *91*, 2519.

[23] Ittel, S. D.; Ibers, J. A. *Adv. Organomet. Chem.* **1976**, *14*, 33.

Downloaded by CARLI CONSORTIUM on June 29, 2009
Published on January 30, 2003 on http://pubs.acs.org | doi: 10.1021/om020815b

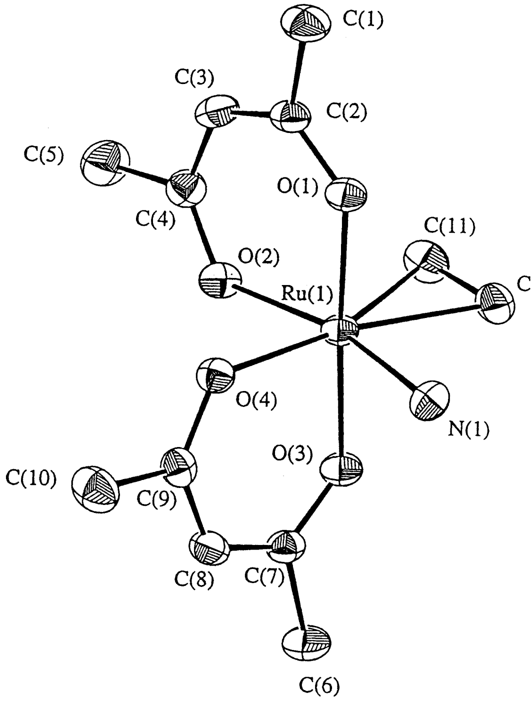

Figure 2. Molecular structure of *cis*-[Ru(acac)$_2$(η^2-C_2H_4)(NH_3)] (*cis*-**8**) with selected atom labeling. Thermal ellipsoids show 30% probability levels; hydrogen atoms have been omitted for clarity.

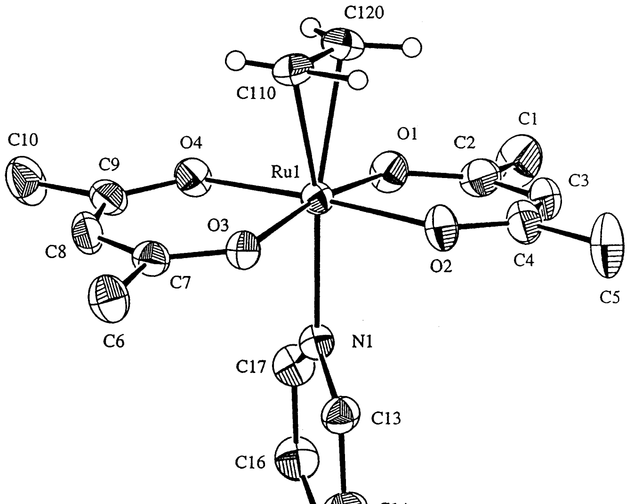

Figure 3. Molecular structure of *trans*-[Ru(acac)$_2$(η^2-C_2H_4)(py)] (*trans*-**9**) with selected atom labeling, showing only the major orientation of the disordered ethene. Thermal ellipsoids show 30% probability levels. Ethene hydrogen atoms are shown as circles of small radii; all others have been omitted for clarity.

(acac)$_2$(*o*-$CH_2{=}CHC_6H_4NMe_2$)] [2.142(2)−2.159(4) Å],[14] probably reflecting the lack of π-acceptor ability of the N-donors and the necessity for the ethene ligands in **5** to compete for d(π)-electron density. The Ru−O distances (2.05−2.09 Å) also are similar to those in the chelate complexes [Ru(acac)$_2$(*o*-$CH_2{=}CHC_6H_4NMe_2$)]. In *cis*-**8** there is evidence for intramolecular hydrogen bonding between two of the acac oxygen atoms, O(1) and O(4), and two ammonia hydrogen atoms [d(O⋯H) = 2.19(3), 2.24(3) Å, N−H⋯O angle = 150 ± 2°].

Table 3. Selected Bond Lengths (Å) and Angles (deg) in *cis*-[Ru(acac)$_2$(η^2-C_2H_4)$_2$] (5)

Ru(1)−O(1)	2.080(1)	Ru(1)−O(2)	2.068(1)
Ru(1)−O(3)	2.061(1)	Ru(1)−O(4)	2.055(1)
Ru(1)−C(11)	2.205(2)	Ru(1)−C(12)	2.209(2)
Ru(1)−C(13)	2.212(2)	Ru(1)−C(14)	2.183(2)
C(11)−C(12)	1.370(3)	C(13)−C(14)	1.353(4)

O(1)−Ru(1)−O(2)	90.32(6)	O(1)−Ru(1)−O(3)	85.87(6)
O(1)−Ru(1)−O(4)	170.05(5)	O(1)−Ru(1)−C(11)	111.64(7)
O(1)−Ru(1)−C(12)	75.63(7)	O(1)−Ru(1)−C(13)	98.47(8)
O(1)−Ru(1)−C(14)	85.18(8)	O(2)−Ru(1)−O(3)	81.56(6)
O(2)−Ru(1)−O(4)	79.86(6)	O(2)−Ru(1)−C(11)	152.77(8)
O(2)−Ru(1)−C(12)	160.95(8)	O(2)−Ru(1)−C(13)	112.26(8)
O(2)−Ru(1)−C(14)	79.25(8)	O(3)−Ru(1)−O(4)	94.21(6)
O(3)−Ru(1)−C(11)	84.11(7)	O(3)−Ru(1)−C(12)	84.60(8)
O(3)−Ru(1)−C(13)	165.35(8)	O(3)−Ru(1)−C(14)	158.74(9)
O(4)−Ru(1)−C(11)	78.24(7)	O(4)−Ru(1)−C(12)	114.29(7)
O(4)−Ru(1)−C(13)	83.92(8)	O(4)−Ru(1)−C(14)	91.35(8)
C(11)−Ru(1)−C(12)	36.17(8)	C(13)−Ru(1)−C(14)	35.85(9)

Table 4. Selected Bond Lengths (Å) and Angles (deg) in *cis*-[Ru(acac)$_2$(η^2-C_2H_4)(NH_3)] (*cis*-8)

Ru(1)−O(1)	2.052(2)	Ru(1)−O(2)	2.066(2)
Ru(1)−O(3)	2.048(2)	Ru(1)−O(4)	2.092(2)
Ru(1)−C(11)	2.147(3)	Ru(1)−C(12)	2.151(3)
Ru(1)−N(1)	2.108(2)	C(11)−C(12)	1.356(4)
C(11)−H(18)	0.94(3)	C(11)−H(19)	1.06(3)
C(12)−H(20)	0.96(3)	C(12)−H(21)	0.97(3)

O(1)−Ru(1)−O(2)	93.07(6)	O(1)−Ru(1)−O(3)	176.67(6)
O(1)−Ru(1)−O(4)	88.28(6)	O(3)−Ru(1)−O(4)	92.79(6)
O(2)−Ru(1)−O(4)	83.68(6)	O(1)−Ru(1)−N(1)	89.74(8)
O(2)−Ru(1)−N(1)	165.43(8)	O(3)−Ru(1)−N(1)	87.29(7)
O(4)−Ru(1)−N(1)	82.12(8)	C(11)−Ru(1)−C(12)	36.8(1)
N(1)−Ru(1)−C(11)	116.0(1)	N(1)−Ru(1)−C(12)	79.2(1)

Table 5. Selected Bond Lengths (Å) and Angles (deg) in *trans*-[Ru(acac)$_2$(η^2-C_2H_4)(py)] (*trans*-9)

Ru(1)−O(1)	2.054(2)	Ru(1)−O(2)	2.046(2)
Ru(1)−O(3)	2.063(2)	Ru(1)−O(4)	2.051(2)
Ru(1)−C(110)	2.171(5)	Ru(1)−C(120)	2.179(5)
Ru(1)−C(111)	2.164(8)[a]	Ru(1)−C(121)	2.179(7)[a]
Ru(1)−N(1)	2.095(3)	C(110)−C(120)	1.35(1)
C(111)−C(121)	1.39(3)	C(110)−C(111)	0.73(2)

O(1)−Ru(1)−O(2)	93.58(9)	O(1)−Ru(1)−O(3)	169.72(9)
O(1)−Ru(1)−O(4)	85.65(9)	O(2)−Ru(1)−O(3)	86.76(8)
O(2)−Ru(1)−O(4)	176.22(9)	O(1)−Ru(1)−N(1)	83.96(9)
C(110)−Ru(1)−C(120)	36.1(3)	C(111)−Ru(1)−C(121)	37.3(7)

[a] Restrained during refinement.

Voltammetry. Cyclic and alternating current (ac) voltammograms of complex **5** show a quasi-reversible electron transfer at $E_{1/2} = +0.95$ V (vs Ag/AgCl) at −50 °C in 0.5 M [Bu_4N]PF_6/CH_2Cl_2, as shown in Figure 4. Although the observed couple is symmetrical, the difference between the potentials of the oxidation and reduction processes was almost twice that found for ferrocene under the same conditions as an internal standard, indicative of slow heterogeneous electron transfer.[24] At room temperature **5** exhibits a chemically irreversible cyclic voltammogram at slow scan rates (ca. 50 mV s^{-1}). A second species, whose behavior was not investigated, was also detected during the reduction process at $E_P = +0.40$ V (vs Ag/AgCl).

The substitution products [Ru(acac)$_2$(η^2-C_2H_4)(L)] (**6**−**9**) show fully reversible voltammograms at −50 °C at a scan rate of 100 mV s^{-1}, the values of $E_{1/2}$($Ru^{3+/2+}$) being in the range +0.37−0.59 V (vs Ag/AgCl) (Table 6). Thus,

---

[24] Astruc, D. *Electron Transfer and Radical Processes in Transition Metal Chemistry*; VCH: New York, 1995.

Downloaded by CARLI CONSORTIUM on June 29, 2009
Published on January 30, 2003 on http://pubs.acs.org | doi: 10.1021/om020815b

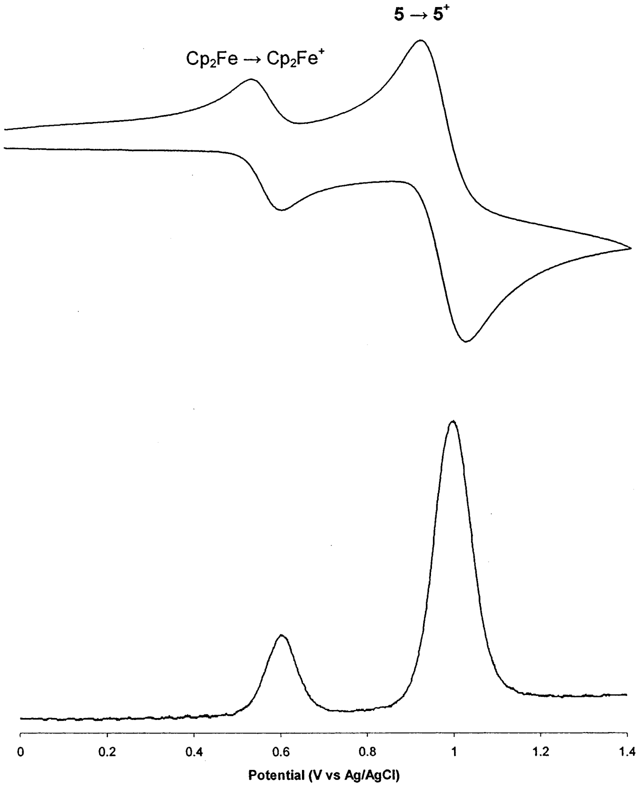

Figure 4. Cyclic (CV) and alternating current (ac) voltammograms for *cis*-[Ru(acac)$_2$(η^2-C_2H_4)$_2$] (**5**) measured at ca. −50 °C in CH_2Cl_2. The scan rates are 100 mV s^{-1} for the CV and 20 mV s^{-1} for the ACV.

Table 6. Reduction Potentials $E_{1/2}$(Ru$^{3+/2+}$) for Complexes [Ru(acac)$_2$(η^2-alkene)(L)]^a

ethene complexes	$E_{1/2}$	cyclooctene complexes	$E_{1/2}{}^b$
5	+0.95	**1**	+0.77
6	+0.59	**2**	+0.44
7	+0.56	**3**	+0.44
trans-**8**	+0.37		
cis-**8**	+0.37	*cis*-**4**	+0.23
trans-**9**	+0.38		

[a] Measured in CH_2Cl_2 at ca. −50 °C vs Ag/AgCl/MeCN. [b] Values from Wallace, L. PhD Thesis, Australian National University, 1991.

replacement of one of the ethene ligands in **5** by L (L = $SbPh_3$, MeCN, NH_3, py) stabilizes Ru(III). The effect is most marked (by 580 mV) for NH_3, which has no π-acceptor ability, and least for $SbPh_3$, which is thought to be a weak π-acceptor.[25] The $E_{1/2}$ values for *cis*- and *trans*-**8** are identical, presumably because C_2H_4 has no competitor for d(π)-electron density, irrespective of the location of the coordinated NH_3. Whereas both *cis*- and *trans*-**8** show fully reversible redox behavior at room temperature, the pyridine complex *trans*-**9** exhibits quasi-reversible behavior at low scan rates under the same conditions, probably because of irreversible loss of ethene. The measured $E_{1/2}$(Ru$^{3+/2+}$) values of the ethene/N-donor complexes **7**−**9** lie in the range +0.38−0.52 V found for the previously reported chelate bidentate N-donor complexes, e.g., $E_{1/2}$ = +0.42, +0.52 V for the diastereomers of [Ru(acac)$_2$(*o*-CH_2=$CHC_6H_4NMe_2$)]$^{0,+1}$.[14] Comparison of the $E_{1/2}$ values of the bis(ethene) complex **5** and the bis(cyclooctene) complex **1** shows the latter to be more easily oxidized to the Ru(III) level by 180 mV, and a similar trend is followed for the corresponding substitution products [Ru(acac)$_2$(η^2-alkene)(L)] (Table 6).

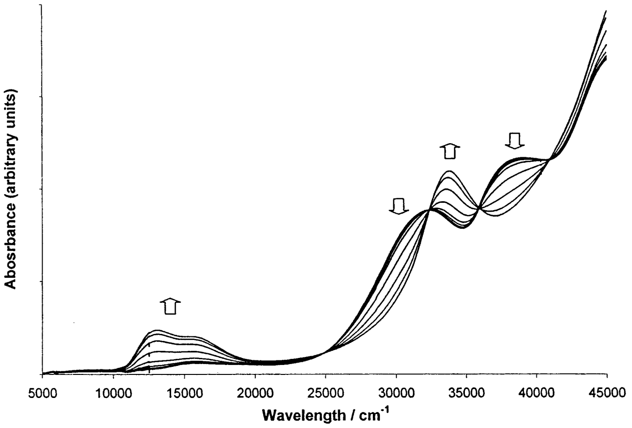

Figure 5. Electronic spectra recorded during the one-electron oxidation of *cis*-[Ru(acac)$_2$(η^2-C_2H_4)$_2$] (**5**) in 0.5 M [Bu_4N]PF_6/CH_2Cl_2 at ca. −50 °C with an applied potential of +1.20 V (vs Ag/AgCl).

Table 7. Principal Electronic Band Maxima (cm^{-1}) and Molar Absorptivities (M^{-1} cm^{-1}) for Ruthenium(II) and in Situ Electrogenerated Ruthenium(III) Complexes

complex	MLCT or LMCT	acac $\pi \rightarrow$ acac π^*
5	32 700 (6000)	38 800 (8000)
6	26 200 (2800)	38 800 (12 600)
trans-**8**	25 000 (2700), 28 500 (4000)	37 700 (14 500)
cis-**8**	25 500 (3100), 31 000 (4900)	36 700 (15 100)
5$^+$	13 300 (2100), 16 000 (1800)	34 100 (8000)
6$^+$	13 900 (1300), 16 900 (1200)	
trans-**8**$^+$	16 000 (1000)	36 000 (8000)
cis-**8**$^+$	16 800 (2200), 27 000 (sh)	34 000 (9800)

Spectroelectrochemistry. The electronic (UV−vis) spectrum of the bis(ethene) complex **5** exhibits a broad band at 32 700 cm^{-1} (ϵ = 6000 M^{-1} cm^{-1}) and a slightly stronger absorption close to 38 800 cm^{-1} (ϵ = 8000 M^{-1} cm^{-1}). When a potential of +1.20 V (vs Ag/AgCl) was applied to the solution at ca. −50 °C, these bands gradually disappeared and new bands appeared at 13 300 cm^{-1} (ϵ = 2600 M^{-1} cm^{-1}), 16 000 cm^{-1} (ϵ = 2200 M^{-1} cm^{-1}), and 34 100 cm^{-1} (ϵ = 8000 M^{-1} cm^{-1}), as shown in Figure 5. After 2−3 h, the solution had been exhaustively oxidized; the original spectrum was regenerated by application of a potential of +0.70 V (vs Ag/AgCl). During both oxidation and reduction, isosbestic points were observed, indicating the presence of only two absorbing species in solution, presumed to be **5** and **5**$^+$.

The electronic spectra recorded at −50 °C for the electro-oxidation of complexes **6**, *trans*-**8**, and *cis*-**8** were similar in their general features to those of **5** and those of the chelate complexes [Ru(acac)$_2$(*o*-CH_2=CHC_6H_4-NMe_2)] reported previously.[14] The band maxima and extinction coefficients are listed in Table 7. At the Ru(II) level there are absorptions at ca. 25 000 and 38 000 cm^{-1}, which are assigned to charge transfer transitions within the Ru(acac)$_2$ unit and acac $\pi \rightarrow \pi^*$ transitions, respectively.[26] On electro-oxidation, these are replaced by a band or bands in the 17 000 cm^{-1} region which probably arise from an acac (π) → Ru(III) MLCT transition; the acac $\pi \rightarrow \pi^*$ transitions in *trans*- and

---

(25) Champness, N. R.; Levason, W. *Coord. Chem. Rev.* **1994**, *133*, 115.

Downloaded by CARLI CONSORTIUM on June 29, 2009
Published on January 30, 2003 on http://pubs.acs.org | doi: 10.1021/om020815b

cis-**8** shift but remain in the 35 000 cm^{-1} region. In the case of **6**, $\pi \rightarrow \pi^*$ transitions of the phenyl rings of Ph_3Sb broaden the spectrum above 30 000 cm^{-1}. As was true for **5**, spectra recorded during the reduction of the electrogenerated Ru(III) species were identical with those of the Ru(II) precursors, showing that these oxidations also are fully reversible.

Bulk anodic electrolysis of *trans*-**8** at −40 °C gave a blue solution whose ESR spectrum in a frozen glass (CH_2Cl_2/THF) at 10 K showed g-values of 1.80 and 2.29, consistent with the presence of a pseudoaxial ruthenium(III) complex. Similar spectra have been reported, for example, for *trans*-$[Ru(NH_3)_4\{P(OEt)_3\}(H_2O)](OTf)_3$ (g = 2.43, 1.68 at 123 K)[27] and *trans*-$[Ru(NH_3)_4\{P(OEt)_3\}_2](OTf)_3$ (g = 2.36, 1.83).[28] Anodic oxidation of **5** under the same conditions as used for *trans*-**8** also formed a deep blue solution, but in situ cyclic voltammetry showed the presence of a second species similar to that detected at room temperature (see above). The ESR spectrum of the frozen solution contained several resonances typical of Ru(III), but the species responsible for them have not been identified.

Since the electrogenerated Ru(III) complexes appeared to be stable indefinitely at −50 °C in solution, we made preliminary attempts to isolate them by chemical oxidation of their Ru(II) precursors. Treatment of *trans*-**8** with a slight deficiency of $[FeCp_2]PF_6$ in CH_2Cl_2 at room temperature gave a mauve solid. Cyclic voltammetry showed the presence of ferrocene, $[Ru(acac)_3]$, and an unidentified species which gave an electrochemically irreversible wave at −0.21 V (vs Ag/AgCl). This product has not been studied further. However, treatment of *trans*-**8** with $AgPF_6$ at −70 °C in CH_2Cl_2 gave a deep blue solution whose ESR spectrum at this temperature showed signals at g = 2.56 and 1.77, similar to those observed in the anodic oxidation of *trans*-**8**; there was also a signal at g = 2.06 of unknown origin. The deep blue solid obtained from the solution rapidly formed a red solution in contact with CH_2Cl_2 at room temperature, and the color of the solid slowly changed to red after a few weeks at −20 °C. The IR spectrum of the blue solid shows typical acac and PF_6 bands,[29] and it seems likely that it is $[Ru(acac)_2(\eta^2\text{-}C_2H_4)(NH_3)]PF_6$, $[\mathbf{8}]^+[PF_6]^-$, but its instability has hindered further characterization.

Since Ru(III) is more stable relative to Ru(II) by 150 mV in the cyclooctene complex *cis*-$[Ru(acac)_2(\eta^2\text{-}C_8H_{14})(SbPh_3)]$ (**2**) than in its ethene analogue **6**, we attempted chemical oxidation of **2**. Treatment with $AgPF_6$ gave a deep blue solid, which appeared to be stable indefinitely at room temperature. Elemental analysis indicated a composition corresponding to $[\mathbf{2}]^+[PF_6]^-$ with ca. 10% $AgPF_6$ contaminant. The positive-ion FAB mass spectrum shows a peak due to the parent ion, together with ions derived by loss of cyclooctene, and the IR spectrum contains the usual O-bonded acac and PF_6 bands. Cyclic and AC voltammetric studies in solution at −45 °C showed a fully reversible Ru^{3+}/Ru^{2+} couple of $E_{1/2} = 0.48$ V (vs Ag/AgCl), which is close to the value found for **2**,[30] and zinc dust reduction regenerated **2**, which was identified by its ^1H NMR spectrum. The ESR spectrum of the blue solid shows g-values at 2.48, ca. 1.98, and 1.83 and is similar in appearance to that reported for the 2-allylpyridine complex *cis*-$[Ru(acac)_2(o\text{-}CH_2{=}CHCH_2C_5H_4N)]^+PF_6^-$.[14] Finally, the UV−vis reflectance spectrum of the isolated solid, measured in a matrix of either KCl or $[Bu_4{}^nN]BF_4$, contains, in addition to a broad, structureless absorption above ca. 25 000 cm^{-1}, a broad band in the region 12 000−18 000 cm^{-1}, which probably corresponds to acac(π) → Ru(III) MLCT transitions (see above); the spectrum of the isolated solid *cis*-$[Ru(acac)_2(o\text{-}CH_2{=}CHC_6H_4NMe_2)]PF_6$,[14] measured under the same conditions, shows a similar band.

Discussion

In contrast to the bis(cyclooctene) complex **1**, the bis(ethene) complex **5** can be isolated and is stable even in the absence of the free olefin. Qualitatively, the relative stabilities are consistent with the binding constants for the two ligands to silver nitrate[31] and with the general observation that alkyl substituents on the olefin tend to decrease the stability of metal-olefin complexes.[31−34] Apart from the cationic aqua complexes $[Ru(H_2O)_5(\eta^2\text{-}C_2H_4)]^{2+}$ [5] and *cis*-$[Ru(H_2O)_4(\eta^2\text{-}C_2H_4)_2]^{2+}$,[5] no other examples of ruthenium(II)-ethene complexes containing only O-donors as the remaining ligands are known. More numerous are those with N-donors, such as $[Ru(NH_3)_5(\eta^2\text{-}C_2H_4)]^{2+}$,[3] $[Ru(porph)(\eta^2\text{-}C_2H_4)]$ (porph = 5,10,15,20-tetra-*p*-tolylporphyrinato dianion or 2,3,7,8,12,13,17,18-octaethylporphyrinato dianion),[35] $[Ru(tmtaa)(THF)(\eta^2\text{-}C_2H_4)]$ (tmtaa = dibenzotetramethyltetraza[14]annulene),[36] and *mer-trans*-$[RuCl_2(\eta^3\text{-}NN'N)(\eta^2\text{-}C_2H_4)]$ [NN′N = 2,6-bis(dimethylamino)pyridine (**10**)[37] or pyridine-2,6-bis(ethylidyne-2,6-dimethylaniline) (**11**)[38]].

In complex **5** the ethene ligands are mutually orthogonal, as is true also for the cationic octahedral bis(ethene) complex **12** derived from **11**[38] and for *cis-mer*-$[OsH(\eta^2\text{-}C_2H_4)_2(PMe_2Ph)_3]^+$.[39] For octahedral bis(ethene) complexes of the type *trans*-$[ML_4(\eta^2\text{-}C_2H_4)_2]$ (M = Mo, L = PMe_3;[40] M = W, L = PMe_3,[41] CO[42]) the rationalization for the observed orthogonal conformation is that it allows back-bonding from two mutually orthogonal

---

[26] The electronic spectra of *trans*- and *cis*-**8** differ mainly in the presence of a band at ca. 28 500 cm^{-1} in the former and at ca. 31 000 cm^{-1} in the latter, which probably arise from a vibronic component of the Ru(II)-acac(π^*) MLCT transition.

(27) de Rezende, N. M. S.; de Castro Martins, S.; Marinho, L. A.; dos Santos, J. A. V.; Tabak, M.; Perussi, J. R.; Franco, D. W. *Inorg. Chim. Acta* **1991**, *182*, 87.

(28) Mazzetto, S. E.; Rodrigues, E.; Franco, D. W. *Polyhedron* **1993**, *12*, 971.

(29) Reference 16, Part A, p 216.

(30) Wallace, L. Ph.D. Thesis, Australian National University, Canberra, 1991.

(31) Muhs, M. A.; Weiss, F. T. *J. Am. Chem. Soc.* **1962**, *84*, 4697.

(32) Cvetanovic, R. J.; Duncan, F. J.; Falconer, W. E.; Irwin, R. S. *J. Am. Chem. Soc.* **1965**, *87*, 1827.

(33) Cramer, R. *J. Am. Chem. Soc.* **1967**, *89*, 4621.

(34) Tolman, C. A. *J. Am. Chem. Soc.* **1974**, *96*, 2780.

(35) Collman, J. P.; Brothers, P. J.; McElwee-White, L.; Rose, E.; Wright, L. J. *J. Am. Chem. Soc.* **1985**, *107*, 4570.

(36) Hessenbrouck, J.; Solari, E.; Scopelliti, R.; Floriani, C.; Re, N. *J. Organomet. Chem.* **2000**, *596*, 77.

(37) del Río, I.; Gossage, R. A.; Hannu, M. S.; Lutz, M.; Spek, A. L.; van Koten, G. *Organometallics* **1999**, *18*, 1097.

(38) Dias, E. L.; Brookhart, M.; White, P. S. *Organometallics* **2000**, *19*, 4995.

(39) Johnson, T. J.; Huffman, J. C.; Caulton, K. G.; Jackson, S. A.; Eisenstein, O. *Organometallics* **1989**, *8*, 2073.

(40) Carmona, E.; Marin, J. M.; Poveda, M. L.; Atwood, J. L.; Rogers, R. D. *J. Am. Chem. Soc.* **1983**, *105*, 3104.

(41) Carmona, E.; Galindo, A.; Poveda, M. L.; Rogers, R. D. *Inorg. Chem.* **1985**, *24*, 4033.

(42) Szymanska-Buzar, T.; Kern, K.; Downs, A. J.; Green, T. M.; Morris, L. J.; Parsons, S. *New J. Chem.* **1999**, *23*, 407.

Downloaded by CARLI CONSORTIUM on June 29, 2009
Published on January 30, 2003 on http://pubs.acs.org | doi: 10.1021/om020815b

Scheme 4

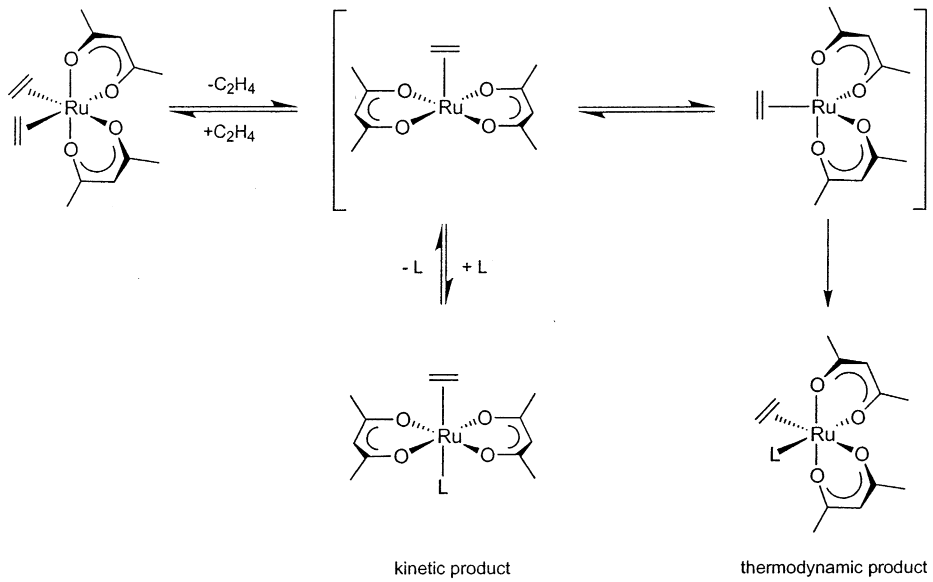

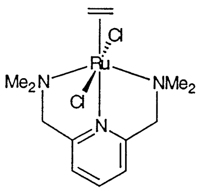

10

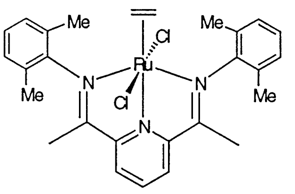

11

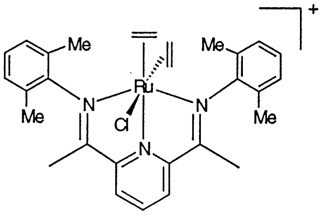

12

metal t_{2g}-derived orbitals to the ethene π*-orbitals, thus reducing the competition for π back-donation. In **5** it is not clear why the orthogonal should be preferred to the parallel arrangement on electronic grounds. Extended Hückel calculations on *cis-mer*-[OsH(η^2-C_2H_4)$_2$(PMe$_2$-Ph)$_3$]$^+$ indicate that the orthogonal arrangement is only ca. 10 kJ/mol more stable than the parallel arrangement;[39] hence, in **5** the outcome may be determined mainly by steric effects. By contrast, in the closely related planar rhodium(I) complex *cis*-[Rh(acac)(η^2-C_2H_4)$_2$] the ethene ligands adopt a parallel arrangement,[43] presumably dictated by both steric effects (no ligands on the *z*-axis) and electronic effects (back-bonding from d_{xz}-, d_{yz}-orbitals).

Unfortunately, the observed equivalence of the carbon nuclei of coordinated ethene, even at −95 °C, precludes an estimate of the barrier to rotation. The implication is either that rotation is very rapid on the NMR time scale, even at the lowest accessible temperature, or that the inequivalence induced by the prochiral *cis*-Ru(acac)$_2$ fragment is unobservably small. The first explanation seems improbable, given that for *cis*-[Rh(acac)(η^2-C_2H_4)$_2$], whose M−C and C═C distances are very similar to those of **5**, the $\Delta G^\ddagger$ value for ethene rotation is 51.7 kJ/mol at 250 K;[44] similar values have been recorded for Pt(II)(acac)-alkene complexes.[45] The variations of the chemical shift of the ethene protons with temperature may result from changes in the population of ethene rotamers; a similar effect has been studied in detail for substituted haloethanes.[46]

In contrast with the behavior of the 16-electron complex [Rh(acac)(η^2-C_2H_4)$_2$], which undergoes rapid intermolecular exchange with ethene at room temperature by an associative mechanism, complex **5** exchanges only slowly with free ethene at room temperature. Reversible dissociation of ethene is probably responsible for the coalescence of the ethene multiplets and of the acac methyl singlets at 80−90 °C. As shown in Scheme 4, it also accounts for the stereochemical course of displacement of one ethene from **5** by ligands. Loss of one ethene molecule from **5** is assumed to generate a square pyramidal intermediate [Ru(acac)$_2$-(η^2-C_2H_4)] in which ethene occupies the apical position. A ligand L should enter preferentially the vacant site, forming the kinetic product *trans*-[Ru(acac)$_2$(η^2-C_2H_4)-(L)], which is observed for L = NH_3 (*trans*-**8**) and L = py (*trans*-**9**). The intermediate [Ru(acac)$_2$(η^2-C_2H_4)] may be interconverting rapidly with a trigonal bipyramidal isomer, e.g., by a Berry pseudorotation about ethene as pivot, and addition of L to this species would generate the thermodynamic product, *cis*-[Ru(acac)$_2$(η^2-C_2H_4)(L)]. The square pyramidal geometry, which is favored on theoretical grounds for five-coordinate d^6 metal complexes,[47,48] has been observed in several ruthenium(II) complexes, e.g., [RuCl$_2$(PPh$_3$)$_3$],[49] [RuCl(NN′N)(PPh$_3$)]-OTf,[50] [Ru(OTf)(NN′N)(PPh$_3$)]OTf[50] (NN′N = 2,6-bis-(dimethylamino)methylpyridine), and [Ru{N(EPR$_2$)$_2$}-

---

[43] Evans, J. A.; Russell, D. R. *Chem. Commun.* **1971**, 197.

[44] Herberhold, M.; Kreiter, C. G.; Wiedersatz, G. O. *J. Organomet. Chem.* **1976**, *120*, 103.

[45] Ashley-Smith, J.; Douek, I.; Johnson, B. F. G.; Lewis, J. *J. Chem. Soc., Dalton Trans.* **1972**, 1776, and earlier papers.

[46] Gutowsky, H. S.; Belford, G. G.; McMahon, P. E. *J. Chem. Phys.* **1962**, *36*, 3353.

[47] Burdett, J. K. *J. Chem. Soc., Faraday Trans. 2* **1974**, *70*, 1599.

[48] Elian, M.; Hoffman, R. *Inorg. Chem.* **1975**, *14*, 1058.

[49] LaPlaca, S. J.; Ibers, J. A. *Inorg. Chem.* **1965**, *4*, 778.

Downloaded by CARLI CONSORTIUM on June 29, 2009
Published on January 30, 2003 on http://pubs.acs.org | doi: 10.1021/om020815b

(PPh_3)] (E = S, Se, R = Ph;[51,52] E = S, R = ^iPr[51]). In the case of [$RuCl_2(PPh_3)_3$], interconversion of the apical and basal PPh_3 ligands is rapid on the ^{31}P NMR time scale at room temperature in solution.[53] Moreover, the addition of ligands to the bis(selenodiphenylphosphoryl)amido complex [Ru{N($SePPh_2$)$_2$}(PPh_3)] resembles that of our bis(alkene)bis(acetylacetonato) complexes in that a mixture of octahedral *trans*- and *cis*-complexes is formed; in the case of hydrazine, the first-formed *trans*-isomer isomerizes to the *cis* form.

The spectroelectrochemical and ESR studies indicate that complexes **5**, **6**, and **8** undergo reversible oxidation to the corresponding Ru(III) cations [Ru(acac)$_2$(η^2-C_2H_4)(L)]$^+$. Although these can be maintained for long periods at −50 °C, most decompose in CH_2Cl_2 at room temperature and are clearly less stable than the Ru(III) complexes formed by chelating olefinic ligands such as 2-vinyl-*N*,*N′*-dimethylaniline, 2-allylpyridine, and 3-butenylmethyl ether.[14] Replacement of one ethene ligand in **5** by the ligand NH_3, MeCN, py, or $SbPh_3$ lowers the $E_{1/2}$($Ru^{3+/2+}$) values from +0.95 V to between +0.37 and +0.59 V (vs Ag/AgCl). The cyclooctene complexes *cis*-[Ru(acac)$_2$(η^2-C_8H_{14})(L)] (**2**−**4**) are more easy to oxidize to the Ru(III) level than their ethene counterparts **6**−**9** by ca. 140 mV; for the bis(alkene) complexes the difference is 220 mV. As mentioned above, alkyl substitution on the double bond tends to weaken alkene coordination at the Ru(II) level, possibly in part by reducing d(π)−π* back-bonding, whereas it may strengthen π−d(σ) bonding at the Ru(III) level.

Exceptionally among the ruthenium(III)-alkene compounds studied, the triphenylstibine complex [Ru(acac)$_2$(η^2-C_8H_{14})($SbPh_3$)]PF_6, [**2**]PF_6, is stable at room temperature, even though in the series [Ru(acac)$_2$(η^2-alkene)(L)]$^+$ (alkene = C_2H_4, C_8H_{14}) the $E_{1/2}$($Ru^{3+/2+}$) values for L = $SbPh_3$ are greater than those for L = NH_3 or py. Since the mode of decomposition of these compounds is not known, further comment on this apparent anomaly is unjustified. However, the observation does suggest that tertiary stibines, which are considered to be moderate σ-donors and also weaker π-acceptors than tertiary phosphines or arsines,[25] could be used to prepare a wider range of stable ruthenium(III)-alkene complexes.

The effect of the acetylacetonate anion relative to the comparable neutral ligands H_2O and NH_3 in stabilizing Ru(III) with respect to Ru(II) in these alkene complexes can be gauged from the $E_{1/2}$($Ru^{3+/2+}$) values. For [Ru(NH_3)$_5$(η^2-C_2H_4)]$^{2+}$ in water, $E_{1/2}$ is reported as +0.93 V vs NHE, whereas for [Ru(acac)$_2$(η^2-C_2H_4)(NH_3)] (**8**) in CH_2Cl_2 the value is +0.37 V vs Ag/AgCl in acetonitrile. A value for **8** in H_2O of +0.23 V vs NHE can be calculated from eq 1 given by Lever,[54] with use of the following values for the electrochemical ligand parameters (E_L) in volts: acac (−0.08), NH_3 (+0.07), and C_2H_4 (+0.76). Thus, substitution of one acac for two ammonia ligands shifts the potential (vs NHE) in favor of Ru(III) by 350 mV. The $E_{1/2}$ value vs NHE for *cis*-[Ru(H_2O)$_4$(η^2-C_2H_4)$_2$]$^{2+}$ in water has not been reported, but a value of +1.57 V can be calculated from eq 1 with use of an E_L value for H_2O of +0.04;[54] the value of $E_{1/2}$ for the very similar diallyl ether complex [Ru(H_2O)$_4$(η^2:η^2-$C_6H_{10}O$)]$^{2+}$ is reported to be greater than 1.5 V.[9] The corresponding value calculated for *cis*-[Ru(acac)$_2$(η^2-C_2H_4)$_2$] (**5**) in water is +1.02 V vs NHE, fortuitously close to the measured value in CH_2Cl_2 vs Ag/AgCl in acetonitrile. Thus, replacement of two water molecules by one acac favors Ru(III) by ca. 270 mV.

$$E_{1/2} = 1.14[\sum E_L(L)] - 0.35 \qquad (1)$$

Experimental Section

General Procedures. All operations were carried out under dry argon with use of standard Schlenk techniques. Hydrocarbon solvents, diethyl ether, and THF were predried over sodium wire and distilled from sodium/benzophenone/tetraglyme under nitrogen. Dichloromethane was dried over CaH_2 and distilled under nitrogen. Zinc dust was washed successively with dilute H_2SO_4, water, and THF and dried under vacuum immediately before use. Industrial grade ethene and anhydrous ammonia were used as received from BOC Gases. The compounds [Ru(acac)$_3$],[55,56] [$FeCp_2$]PF_6,[57] and *cis*-[Ru(acac)$_2$(η^2-C_8H_{14})($SbPh_3$)] (**2**)[13] were prepared by published methods.

Reactions with ethene were carried out in a glass Lab Crest medium-pressure vessel (90 mm height by 50 mm width) in a hood behind a safety screen.

NMR spectra were recorded at 20.5 °C (unless otherwise indicated) on Varian Gemini 300 BB or VXR 300 spectrometers (^1H at 300 MHz, ^{13}C at 75.4 MHz). Variable-temperature NMR spectra were recorded on the Varian VXR 300 instrument. The chemical shifts (δ) for ^1H and ^{13}C are given in ppm referenced to the residual protons and the carbon atoms of the deuterated solvents. Coupling constants (J) are given in hertz (Hz). Infrared spectra were recorded on either a Perkin-Elmer 1800 FT or a Perkin-Elmer Spectrum One instrument with use of KBr disks or 0.1 mm path length KBr cells. Fast atom bombardment (FAB) mass spectra were measured on a VG ZAB2-SEQ spectrometer using either 3-nitrobenzyl alcohol or (3-nitrophenyl)octyl ether as the matrix. Microanalyses were performed in-house.

Electrochemical measurements in CH_2Cl_2 at various temperatures were performed on a Princeton Applied Research 170 system as described elsewhere[58] linked to a Macintosh LC630 computer via an AD Instruments MacLab interface system. Peak-to-peak separations in cyclic voltammetry (CV) and peak widths in alternating current voltammetry (ACV) were assessed for electrochemical reversibility by comparison with [$FeCp_2$]$^{+/0}$ at the same peak current. At room temperature $E_{1/2}$($Fe^{3+/2+}$) for this couple was +0.55 V vs a nonaqueous reference electrode consisting of Ag/AgCl/MeCN/0.5 M [Bu_4N]PF_6. Typical scan rates for CV were 50−500 and 20 mV s^{-1} for ACV.

Electronic spectra in the range 6000−45 000 cm^{-1} were collected by use of a cryogenically controlled, optically transparent thin-layer electrode (OTTLE) cell placed in the beam of either a Perkin-Elmer Lambda 9 or a Cary 5E UV−vis−NIR spectrophotometer as described previously.[58] The same

---

[50] Abbenhuis, R. A. T. M.; del Río, I.; Bergshoef, M. M.; Boersma, J.; Veldman, N.; Spek, A. L.; van Koten, G. *Inorg. Chem.* **1998**, *37*, 1749.

[51] Leung, W. H.; Zheng, H.; Chim, J. L. C.; Chan, J.; Wong, W. T.; Williams, I. D. *J. Chem. Soc., Dalton Trans.* **2000**, 423.

[52] Zhang, Q. F.; Zheng, H. G.; Wong, W. Y.; Wong, W. T.; Leung, W. H. *Inorg. Chem.* **2000**, *39*, 5255.

[53] Hoffman, P. R.; Caulton, K. G. *J. Am. Chem. Soc.* **1975**, *97*, 4221.

[54] Lever, A. B. P. *Inorg. Chem.* **1990**, *29*, 1271.

[55] Johnson, A.; Everett, G. W., Jr. *J. Am. Chem. Soc.* **1972**, *94*, 1419.

[56] Earley, J. E.; Base, R. N.; Berrie, B. H. *Inorg. Chem.* **1983**, *22*, 1836.

[57] Brauer, G. *Handbuch der Präparativen Anorganischen Chemie*; Ferdinand Enke: Stuttgart. Germany, 1981; Vol. 3, p 1845.

[58] Duff, C. M.; Heath, G. A. *Inorg. Chem.* **1991**, *30*, 2528.

Downloaded by CARLI CONSORTIUM on June 29, 2009
Published on January 30, 2003 on http://pubs.acs.org | doi: 10.1021/om020815b

solution was prepared and transferred to the sample cell in an argon-filled Braun Labmaster 130 glovebox. The electrolysis was carried out at a potential typically 300 mV past the appropriate $E_{1/2}$ value and continued until the spectrum changed no further and the current had decayed to a constant minimum. The potential was then reset, and the spectrum of the starting complex was regenerated. The observation of sharply defined isosbestic points and the full regeneration of the starting spectra were taken as evidence that the process was chemically reversible.

Continuous wave X-band ESR spectra were collected on a Bruker ESP 300e spectrometer with a rectangular TE102 cavity and a frequency counter for accurate *g*-value measurements. The following settings were used: modulation frequency 50−100 kHz, microwave power 2.0 mW (sufficiently low to avoid sample saturation), modulation amplitude 5 G, time constant 0.33 s, and sweep time 330 s. The temperature was lowered to 4.8 K with liquid helium and an Oxford Instruments cryostat.

Elemental analyses, selected IR bands, and mass spectrometric data are collected in Table 1.

Preparations. *cis*-[Ru(acac)$_2$(η^2-C$_2$H$_4$)$_2$] (5). Freshly activated zinc dust (2.4 g, 36.7 mmol) was mixed with Ru(acac)$_3$] (930 mg, 2.34 mmol) in a medium-pressure vessel that was evacuated and backfilled with ethene (1 bar) three times. Freshly distilled THF (20 mL) and ca. 12 drops of deoxygenated, distilled water were added to the mixture via syringe. The flask was then heated to ca. 80 °C with magnetic stirring under 3 bar of ethene pressure (**CAUTION:** a safety shield was used when the pressure of the vessel was higher than 1 bar). Within 1 h, the solution changed color from cherry-red to dark brown and finally became orange.

After allowing the reaction vessel to cool to room temperature and reducing the pressure to 1 bar, the heterogeneous reaction mixture was allowed to stand for ca. 10 min. The zinc dust quickly settled on the bottom of the flask, and the cloudy solution was carefully decanted into a Schlenk flask under an ethene atmosphere (1 bar). The solvent was removed in vacuo, and the orange residue was treated with pentane (10 mL). The solution was separated from a white colloidal suspension, presumably containing zinc(II) byproducts, by filtration through a short column (ca. 5 × 2 cm) of neutral alumina (Activity III) under C_2H_4 (1 bar). Elution successively with *n*-pentane and benzene gave a clear orange solution. The solvent was removed in vacuo, and the minimum amount of pentane (ca. 5 mL) was added to redissolve the residue. After 2 days at −20 °C, 500 mg (60%) of orange, microcrystalline **5** was isolated and washed carefully with cold pentane. Crystals suitable for X-ray diffraction studies were obtained by slow evaporation of the supernatant.

***cis*-[Ru(acac)$_2$(η^2-C$_2$H$_4$)(SbPh$_3$)] (6).** A solution of SbPh$_3$ (412 mg, 1.17 mmol) in THF (40 mL) was added dropwise to a THF solution (ca. 40 mL) of **5** (prepared from [Ru(acac)$_3$] (500 mg, 1.26 mmol)), and the mixture was stirred overnight at room temperature to give a brown solution. The solvent was removed in vacuo. The brown residue was extracted with benzene or toluene and chromatographed on a neutral alumina column (Activity III). The yellow band that eluted first was immediately pumped to dryness to give a brownish oil. On stirring with pentane (150 mL) for 45 min, complex **6** formed as an air-stable yellow solid (537 mg, 63%), which was isolated by filtration. The ^{1}H NMR spectrum of **6** showed the presence of a small amount of *cis*-[Ru(acac)$_2$(SbPh$_3$)$_2$],[13] which could not be removed by fractional crystallization.

***cis*-[Ru(acac)$_2$(η^2-C$_2$H$_4$)(MeCN)] (7).** A solution of **5** was prepared from [Ru(acac)$_3$] (360 mg, 0.90 mmol) in THF (20 mL) and stirred with acetonitrile (0.2 mL, 4.1 mmol) at room temperature overnight. The mixture was evaporated to dryness, and the residue was stirred with hexanes (ca. 10 mL) for 20 min to leave **7** as an air-stable, yellow-brown solid (250 mg, 75%).

***trans*-[Ru(acac)$_2$(η^2-C$_2$H$_4$)(NH$_3$] (*trans*-8).** When ammonia gas was bubbled through a solution of **5** (prepared from [Ru(acac)$_3$], (1.25 g, 3.15 mmol)) in THF for 20 min, an orange precipitate formed. The solvent was removed in vacuo, and the solid was washed several times with hexanes. The yield of *trans*-**8** was 670 mg (62%).

***cis*-[Ru(acac)$_2$(η^2-C$_2$H$_4$)(NH$_3$)] (*cis*-8).** A solution of *trans*-**8** prepared as above from [Ru(acac)$_3$] (607 mg, 1.52 mmol) in CH$_2$Cl$_2$ (ca. 2 mL) was chromatographed on neutral alumina (Activity III). The first red fraction that eluted with CH$_2$Cl$_2$ was discarded. An orange fraction was collected and evaporated to dryness in vacuo. The residue was stirred with *n*-pentane (20 mL), leaving *cis*-**8** as a yellow-brown microcrystalline solid. The yield was 230 mg (45%). Crystals suitable for X-ray diffraction were obtained by slow evaporation of the supernatant. Both *cis*- and *trans*-**8** are stable as solids when exposed to air for several months.

***trans*- and *cis*-[Ru(acac)$_2$(η^2-C$_2$H$_4$)(py)] (9).** A solution of **5** in toluene (20 mL) that had been freshly prepared from [Ru(acac)$_3$] (395 mg, 0.99 mmol) was treated with pyridine (80 μL), and the mixture was stirred at room temperature for 3 h. The orange solution was evaporated in vacuo to ca. 1 mL volume, layered with hexanes, and set aside at 0 °C. An X-ray quality crystal selected from those that deposited first (ca. 50 mg) proved to be *cis*-**9**. The total yield of **9** as a 3:2 *cis*/*trans* mixture was 362 mg (70%).

Attempted Oxidation of *trans*-8. A solution of *trans*-**8** (105 mg, 0.31 mmol) in CH$_2$Cl$_2$ (10 mL) was cooled to −70 °C, and AgPF$_6$ (105 mg, 0.41 mmol) was added. The deep blue solution was stirred for 1 h at this temperature, filtered through Celite contained in a column cooled in dry ice, and evaporated in vacuo to give a blue solid, which was stirred with cold ether for 2 h. The solid is believed to be [**8**]$^+$[PF$_6$]$^-$ (see text).

Oxidation of *cis*-[Ru(acac)$_2$(η^2-C$_8$H$_{14}$)(SbPh$_3$)] (2). A solution of **2** (330 mg, 0.43 mmol) in CH$_2$Cl$_2$ (10 mL) was cooled to −70 °C and treated with AgPF$_6$ (165 mg, 0.65 mmol). Workup as described above gave [**2**]$^+$[PF$_6$]$^-$ (316 mg, 80%) as a blue solid that appeared to survive in air at room temperature over a period of months.

Voltammetry. The difference between the potentials of the oxidation and reduction processes, ΔE_P (mV), for **5** at −50 °C varied with scan rate (mV s^{-1}, in parentheses), as follows: 90 (50), 106 (100), 122 (200), and 160 (500). Under the same conditions, ferrocene showed values of 62 (50), 64 (100), 66 (200), and 85 (500).

X-ray Crystallography. Crystal data and details of data collection are given in Table 8. The data for complex **5** were collected on a Nonius Kappa CCD area detector (graphite monochromated Mo Kα radiation, $\lambda = 0.71069$ Å) and processed with use of the computer programs Denzo and Scalepak.[59] The structure was solved by heavy-atom Patterson methods,[60] expanded with use of Fourier techniques,[61] and refined by full-matrix least squares, the function minimized being $\sum w(|F_o| - |F_c|)^2$.

The data for *cis*-**8** were collected on a Rigaku AFC6S diffractometer employing graphite-monochromated Mo Kα radiation, $\lambda = 0.71069$ Å, and $\theta - 2\theta$ scans. The cell parameters were determined by least-squares fitting of 25 carefully centered reflections in the range 49.74° < 2θ < 54.85°. The

---

(59) Otwinowsky, Z.; Minor, W. In *Methods in Enzymology*; Carter, C. W., Jr., Sweet, R. M., Ed.; Academic Press: New York, 1997; Vol. 276, pp 307−326.

(60) PATTY: Beurskens, P. T.; Admiraal, G.; Beurskens, G.; Bosman, W. P.; Garcia-Granda, S.; Gould, R. O.; Smits, J. M. M.; Smykalla, C. *The DIRDIF-92 Program System*; Technical Report of the Crystallography Laboratory; University of Nijmegen: Nijmegen, The Netherlands, 1992.

(61) Beurskens, P. T.; Admiraal, G.; Beurskens, G.; Bosman, W. P.; de Gelder, R.; Israel, R.; Smits, J. M. M. *The DIRDIF-94 Program System*; Technical Report of the Crystallography Laboratory; University of Nijmegen: Nijmegen, The Netherlands, 1994.

Downloaded by CARLI CONSORTIUM on June 29, 2009
Published on January 30, 2003 on http://pubs.acs.org | doi: 10.1021/om020815b

Table 8. Crystal and Refinement Data for $[Ru(acac)_2(\eta^2\text{-}C_2H_4)_2]$ (5), *cis*-$[Ru(acac)_2(\eta^2\text{-}C_2H_4)(NH_3)]$ (*cis*-8), and *trans*-$[Ru(acac)_2(\eta^2\text{-}C_2H_4)(py)]$ (*trans*-9)[a]

	5	*cis*-**8**	*trans*-**9**
empirical formula	$C_{14}H_{22}O_4Ru$	$C_{12}H_{21}NO_4Ru$	$C_{17}H_{23}NO_4Ru$
fw	355.40	344.37	406.44
cryst syst	triclinic	monoclinic	monoclinic
space group	$P\bar{1}$ (No. 2)	$P2_1/n$ (No. 14)	$P2_1/n$ (No. 14)
cryst color, habit	yellow, plate	orange, plate	orange, plate
a (Å)	7.6278(2)	11.869(3)	8.340(1)
b (Å)	8.9725(4)	10.400(4)	17.307(1)
c (Å)	12.5027(5)	12.247(2)	13.026(1)
α (deg)	76.719(2)		
β (deg)	74.620(2)	103.26(1)	99.324(9)
γ (deg)	70.659(2)		
V (Å^3)	768.78(3)	1471.5(5)	1855.3(3)
Z	2	4	4
D_{calc} (g cm^{-3})	1.535	1.554	1.455
μ (cm^{-1})	10.27	10.49	71.42
T (K)	200	296	243
cryst dimens (mm)	0.20 × 0.20 × 0.10	0.38 × 0.29 × 0.08	0.27 × 0.19 × 0.08
F(000)	364	704	832
$2\theta_{max}$ (deg)	55.1	55.1	120.1
no. of reflns measd	8834	3755	5970
no. of unique reflns	3476 (R_{int} = 0.028)	3589 (R_{int} = 0.012)	2761 (R_{int} = 0.044)
no. of observations	3285 [$I > 2\sigma(I)$]	2713 [$I > 2\sigma(I)$]	2551 [$I > 2\sigma(I)$]
no. of variables	196	226	227
p-factor	0.040	0.020	0.020
R; R_w	0.025; 0.035	0.021; 0.022	0.028; 0.031
GOF	1.23	1.33	1.83
ρ_{max}, ρ_{min} (e Å^{-3})	0.44; −0.96	0.28; −0.30	0.71; −0.58

[a] Definitions: $R = \Sigma||F_o| - |F_c||/\Sigma|F_o|$; $R_w = [\Sigma w(|F_o| - |F_c|)^2/\Sigma wF_o^2]^{1/2}$; $w = [\sigma^2(F_o) + 0.25p^2F_o^2]^{-1}$; GOF $= [\Sigma w(|F_o| - |F_c|)^2/(N_o - N_v)]^{1/2}$, where N_o = number of observations, N_v = number of variables.

structure was solved by direct methods[62] and expanded and refined as described for **5**.

The data for *trans*-**9** were collected on a Rigaku AFC6R diffractometer with graphite-monochromated Cu Kα radiation, $\lambda = 1.54178$ Å, and $\theta-2\theta$ scans. The cell parameters were determined from a least-squares refinement of 23 carefully centered reflections in the range 109.23° < 2θ < 109.82°. The structure was solved, expanded, and refined as described for **5**.

The non-hydrogen atoms of **5** and *cis*-**8** were refined anisotropically. For **5** the acac hydrogen atoms were included at geometrically determined positions which were periodically recalculated but not refined, the methyl groups being aligned to best-fit peaks in difference electron density maps. The ethene hydrogen atoms were located in difference maps, and their coordinates were refined. For *cis*-**8** the hydrogen atoms were located in inner-data difference electron density maps, but their isotropic B-values were kept fixed. In *trans*-**9** the coordinated ethene was disordered over two orientations that were at approximately 90° to each other. The relative populations of the two orientations were refined. Restraints were imposed on the Ru−C distances of the minor orientation to keep them nearly equal. These atoms were refined with isotropic displacement factors fixed at the average value of B_{eq} of the other two ethene carbon atoms; all other non-hydrogen atoms were refined anisotropically. With the exception of those on the ethene, all hydrogen atoms were treated as described above for **5**. Four peaks were observed close to the ethene carbon atoms, apparently corresponding to the ethene hydrogen atoms. The expected hydrogen atom sites for the two ethene orientations are almost coincident. These four peaks were therefore incorporated in the structure as hydrogen atoms of full occupancy and were refined positionally. However, the associated distances and angles are not reliable because each is, at best, a weighted average of two sites.

Neutral atom scattering factors were from ref 63. Anomalous dispersion effects were included in F_C,[64] the $\Delta f'$ and $\Delta f''$ values and mass attenuation coefficients being from refs 65 and 66, respectively. Calculations were performed with use of the maXus[67] (for **5**) and teXsan[68] (for **5**, *cis*-**8**, and *trans*-**9**) programs.

Acknowledgment. We thank Dr. Richard Webster for the ESR measurements, Dr. Guandolina Chung and Mr. Horst Neumann for preliminary preparative experiments, Dr. Graham Heath for assistance with the electrochemical measurements and helpful discussions, and Johnson-Matthey Co., UK, for the loan of hydrated ruthenium chloride.

Supporting Information Available: Tables giving X-ray data for **5**, *cis*-**8**, and *trans*-**9**. This material is available free of charge via the Internet at http://pubs.acs.org.

OM020815B

---

(62) SIR 92: Altomare, A.; Cascarano, M.; Giacovazzo, C.; Guagliardi, A.; Burla, M. C.; Polidori, G.; Camalli, M. *J. Appl. Crystallogr.* **1994**, *27*, 435.

(63) Cromer, D. T.; Waber, J. T. *International Tables for X-ray Crystallography*; Kynoch Press: Birmingham, England, 1974; Vol. IV.

(64) Ibers, J. A.; Hamilton, W. C. *Acta Crystallogr.* **1964**, *17*, 781.

(65) Creagh, D. C.; McAuley, W. J. *International Tables for Crystallography*; Kluwer Academic: Boston, MA, 1992; Vol. C, p 219.

(66) Creagh, D. C.; Hubbell, J. H. *International Tables for Crystallography*; Kluwer Academic: Boston, MA, 1992; Vol. C, p 200.

(67) maXus: Mackay, S.; Gilmore, C. J.; Edwards, C.; Stewart, N.; Shankland, K. *Program for the Solution and Refinement of Crystal Structures*; Nonius, Delft, MacScience, Japan, and the University of Glasgow, 1999.

(68) *teXsan*: *Single-Crystal Structure Analysis Software*, Version 1.8; Molecular Structure Corp.: The Woodlands, TX, 1997.